nzsee
NEW ZEALAND SOCIETY FOR EARTHQUAKE ENGINEERING

Numerical modelling of reinforced concrete walls with minimum vertical reinforcement contents

T. Deng, R.S. Henry
Department of Civil and Environmental Engineering, University of Auckland, Auckland.

ABSTRACT

Reinforced concrete (RC) structural walls are effective lateral force-resisting components that are commonly implemented in tall buildings. Recent studies have investigated the impact of minimum vertical reinforcement limits on the ductility at the plastic hinge region of RC walls and resulted in revisions to design standard requirements in both New Zealand and the United States. These studies focused on rectangular walls with a clear plastic hinge region at the wall base, whereas tall buildings exhibit more distributed plasticity demands up the wall height. In order to investigate the tall wall performance designed in accordance with the current standard, distributed plasticity beam-column fiber element was implemented to simulate the behaviour of the walls. The modelling technique was validated against the experimental tests with a range of vertical reinforcement contents to ensure a full range of wall sections can be accurately modelled. Following calibration and validation of the model, a push-over analysis was conducted on a 10-storey wall satisfying the minimum vertical reinforcement requirement over the full wall height to understand the wall critical section performance where the required additional reinforcement in the plastic hinge region terminates. The result obtained from this numerical study illustrated the upper storeys with the minimum required vertical reinforcement above intend plastic height are susceptible to unintended concentrations in in-elastic demands and fracture of vertical reinforcement.

1 INTRODUCTION

Reinforced concrete structural walls are commonly selected as lateral load-resisting components in tall buildings. Recent studies have investigated the impact of minimum vertical reinforcement limits on the ductility within the clear plastic hinge region at wall base. For instance, tests of walls with minimum reinforcement contents highlighted the non-ductile and limited ductile response for the walls designed in accordance with ACI 318-14 vertical reinforcement limits (Puranam & Pujol, 2017). The test walls designed in accordance with revised minimum vertical reinforcement limits in NZS 3101:2006 (A3) indicated that additional reinforcement at the ends of the wall was capable of generating well-distributed secondary cracks

to achieve the targeted ductility (Lu, Gultom, Ma, & Henry, 2018). However, tall buildings exhibit more distributed plasticity demand up the wall height because of the higher modes effects (R.W.G.Blakeley, R.C.Cooney, & L.M.Negget, 1975), (Priestley, Calvi, & Kowalsky, 2007), (Panagiotou & Restrepo, 2009). The termination of reinforcement above the well-detailed hinge region at wall base and amplified bending moment lead to the occurrence of yielding up to the full wall height, where the reinforcement content may not be sufficient to ensure a ductile response is achieved.

In order to extend the previous research into minimum vertical reinforcement limits, an investigation of the seismic response of tall RC walls with minimum vertical reinforcement was initiated. A modelling technique for RC tall walls was developed that consists of displacement based fiber elements in OpenSees with a regularisation technique implemented to accurately capture strain localisation and wall failure. The modelling technique was validated against the experimental tests with a range of vertical reinforcement contents to ensure the full range of wall sections can be accurately modelled. The model was then used to investigate a 10-storey tall wall satisfying the minimum vertical reinforcement requirement over the full wall height.

2 MODEL DESCRIPTION

The model verification aimed to develop efficient approaches to simulate the seismic behaviour of RC walls across a range of vertical reinforcement contents. Distributed plasticity beam-column fiber elements have been extensively investigated and applied to simulate the flexural behaviour of RC components (Spacone, Filippou & Taucer, 1996) (Pugh, 2012). Among a wide variety of fiber models, force-based element (FBE) and displacement-based element (DBE) are the two primary formulations used to simulate the nonlinear response of RC walls. Both of the models permit the plastic hinge forming at any location along with the wall height through the integration of the force-deformation response at sections along the individual element length. DBE method follows the standard finite element approach where the element deformation equilibrium based upon the interpolation of nodal displacement. In FBE, a linear moment distribution is assumed along with the element that can represent a reliable nonlinear response. When a sufficiently refined meshing scheme is used, element number in DBE and integration point number in FBE, both can be successfully used in the nonlinear analysis to achieve comparable response to that of previously test walls. However, in dynamic time-history analysis, DBE performs better convergence characteristics compared to FBE (Marafi, Ahmed, Lehman, & Lowes, 2019). As a series of time history analysis was planned to conduct in a follow-up study, the DBE was selected for this study.

Regularisation is a fundamental procedure for investigating a mesh objective response in fiber models, because of the characteristic length in the finite element discretisation. Two primary methods were generalised to address the localisation issues in the simulation, representative in the modification of the material stress-strain properties (J， Coleman; & Spacone, 2001) and the selection of the appropriate integration scheme (Scott & Fenves, 2006), (Scott & Ryan, 2013). In this study, a thorough method of localisation characteristic for the material properties was developed for the application of nonlinear analysis. For the wall designed with the minimum vertical reinforcement requirement, the cracking of concrete and fracture of reinforcement is representative for the tension failure. In order to minimise the effect of element length on the strain localisation for the lightly reinforcement wall, a constant post-yield energy approach was adopted to regularise the reinforcement ultimate strain using the experimental stress-strain energy envelop (Pugh, 2012). Although the strain regularisation defines the reinforcement tension deformation limitation, the ultimate stress affected by the hardening slope is an essential factor to represent the strength capacity within the hardening stage. The integrated application for both strain and developed stress regularisation was proposed to predict the RC components dominated by tension failure. Equation 1 was proposed for regularising the strain-hardening slope to determine the ultimate stress that based upon the constant energy

assumption, where E_s is the initial elastic slope, b is hardening slope coefficient, bE_s is the strain-hardening slope, G_s is the post yielding energy, ε_u is ultimate strain, ε_y is the yield strain, and f_y is the yield stress. For concrete property, the tensile softening stiffness is another significant factor that affects the response of failure of lightly reinforced RC walls. Equation 2 was proposed for regularising the softening stiffness after tensile cracking, where G_f is the concrete tensile cracking energy, f_{cr} is the concrete tensile strength, L_{ele} is the calculated element length.

$$bE_s = \frac{2 \times G_s}{L_{IP} \times (\varepsilon_u - \varepsilon_y)} - \frac{2 \times f_y}{(\varepsilon_u - \varepsilon_y)} \quad (1)$$

$$E_{ts} = \frac{f_{cr}}{\varepsilon_{ts} - \varepsilon_{cr}} = \frac{f_{cr}^2 \times L_{ele}}{2 \times G_f} \quad (2)$$

The fiber element couples the axial and flexural response of the section but ignores the shear response. In order to account shear deformations of wall elements, the additional zero-length element representing the shear spring was introduced into the model. The equivalent linear elastic shear stiffness was estimated as Equation 3, where k_s is the uncracked shear stiffness, G is shear modulus, A_s is 80% of the gross section area and h_l is the tributary length of the shear springs. The constant shear stiffness definition had been proved for the availability by the means of C shape wall experiments (Beyer, 2007) (Arabzadeh & Galal, 2017).

$$K_s = \frac{GA_s}{h_l} \quad (3)$$

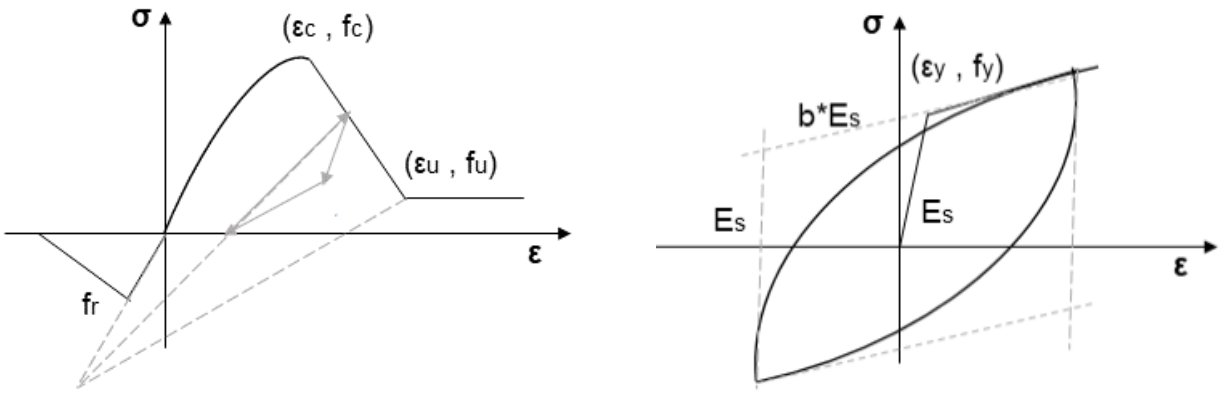

(a) Schematic Concrete02 stress-strain curve **(b) Schematic Steel02 stress-strain curve**

Figure 1: Constitutive material models

Uniaxial constitutive material models were used to represent the nonlinear material behaviour within the fiber element sections, and the P-Delta formulation was applied to describe the nonlinear geometric response. A modified Kent-Park concrete model (Yassin Mohd, 1994) was used to capture the nonlinear behaviour (available in OpenSees as Concrete02). The Concrete02 is capable of providing a reasonable and comprehensive result that extensively used in RC wall simulation (Orakcal, Massone, & Wallace, 2006), (Encina & Henry, 2015). The compressive behaviour of Concrete02 is expressed by three regions, including an ascending parabolic branch, a descending linear branch and a constant residual strength. The tensile behaviour is defined by a bi-linear curve with zero residual strength, as shown in Figure 1a. The tensile strength was calculated as 0.3 $(f_{ck})^{2/3}$ in accordance with the fib Model code, where f_{ck} is the characteristic compressive strength (fib Bulletin 65, 2012). For steel reinforcement, the Giuffré-Menegetto-Pinto hysteretic model in OpenSees defined as Steel02 was selected (Filippou, Popov & Beryero, 1983). The Steel02 model describes the stress-strain relation for a linear elastic curve with the slope E_s as the initial elastic modulus.

Subsequently, the hardening slope with an introduced coefficient is expressed as bE_s to describe the behaviour after the yielding point, as shown in Figure 1 b. The asymptote for the initial elastic and hardening curve represents the Bauschinger effect during the unload and reload stage. There is no regularisation function built into Steel02, and so the MinMax material command was coupled to use to define the tension and compression strain limitation in the stress-strain response. Once the limits were triggered, the reinforcement stress immediately drops to zero. The material was assigned to the corresponding fibre region according to the actual position in the wall cross-section, and no bond-slip effect is concerned for the reinforcement and concrete interaction in the model.

3 MODEL COMPARISON AND VALIDATION

3.1 Walls W1-60-0.14 and W-60-0.24 (ACI 318-14)

Wall W1-60-0.14 and W1-60-0.24 were part of the test program to investigate the response of very lightly reinforced concrete walls (Puranam & Pujol, 2017). The test members were designed with minimum vertical reinforcement of 0.15% for the ordinary wall and 0.25% for the special wall in accordance with ACI 318-14 (ACI Committee 318, 2014).

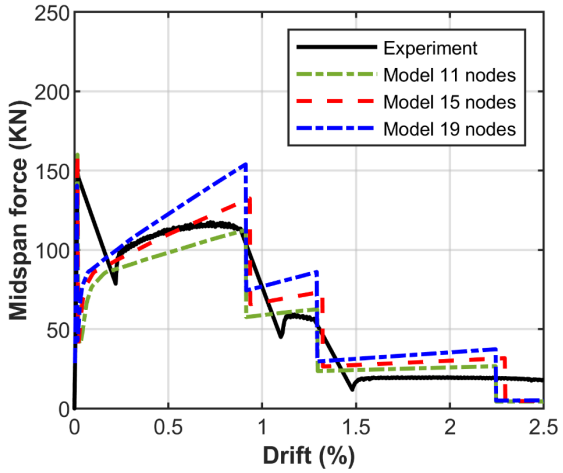

(a) Wall W1-60-0.14 with partial regularization

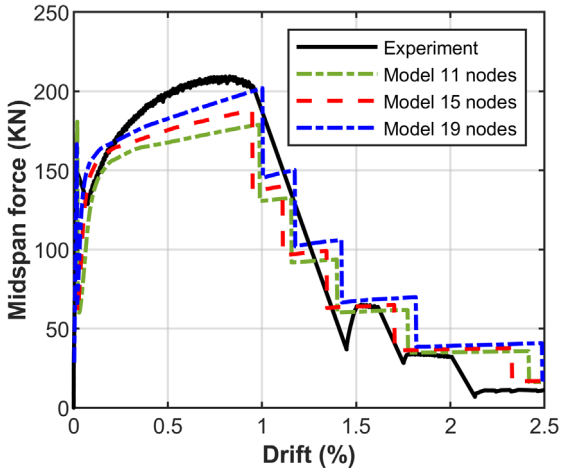

(b) Wall W1-60-0.25 with partial regularization

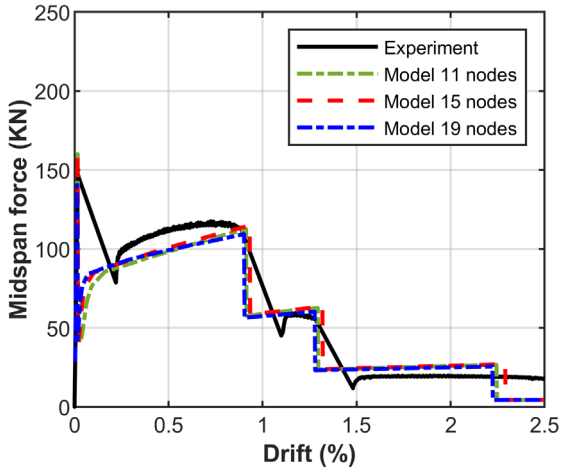

(c) Wall W1-60-0.14 full regularization

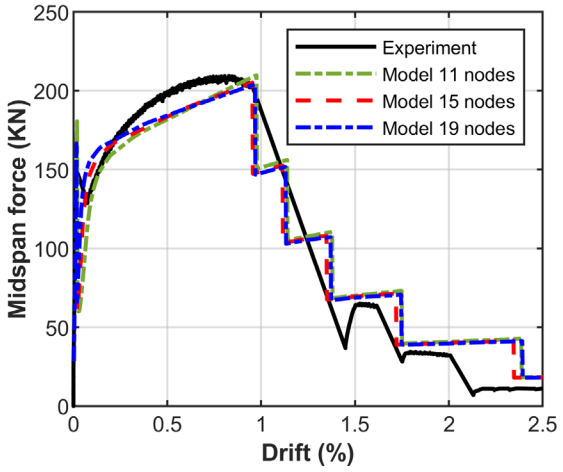

(d) Wall W1-60-0.25 with full regularization

Figure 2: Comparison of the proposed model with partial and full regularization technique and the experiment Wall W1-60-0.14 and W1-60-0.24

The model developed was compared against these test results to verify the proposed regularisation method and element number sensitivity for the lightly reinforced concrete walls. Models with the equal length element that consisted of 11, 15 and 19 nodes to exhibit the cracking behaviour for lightly reinforcement test walls. Figure 2 a & b illustrated the partial regularisation that included adjusting only the ultimate strain of the reinforcement material was generally able to capture the wall behaviour but failed to provide an accurate or consistent calculation of ultimate strength. The full regularisation with the incorporated strain and stress regularisation was able to match the experimental result with acceptable accuracy in respect of the cracking strength, ultimate strength and drift capacity at reinforcement fracture, as depicted in Figure 2 c & d. The test and model results both showed the wall specimens displayed a sudden drop in load after the first cracking. For 0.15% reinforcement ratio wall specimen, the ultimate strength was approximately 80% of the strength prior to cracking with the wall never fully recovering the tensile strength released when the first crack formed. The 0.25% reinforcement ratio specimen dipped temporarily after the first cracking and the ultimate strength prior to reinforcement fracture exceeded the cracking strength. However, the drift ratio of less than 1% indicated the upper wall portion designed with the reinforcement content only likely to achieve a limited ductile response. There was some discrepancy in the calculated response after cracking with a steeper descending slope calculated by the model compared to the test response. This is due to the rapid-strength drop not being able to be recorded with sufficient sampling speed during the testing. The loading rig was failed to capture the sufficient amount of data from the concrete cracking to the recovery of strength period. In contrast, the recorded response in the numerical model depends on the calculated increment and tolerance for each step, The quantitive data, herein, can be acquired from the modelling result to describe the behaviour after the initial cracking.

3.2 Walls C1 and M5 (NZS 3101:2006-A2/A3)

Walls C1 and M5 were part of a test program to investigate the ductility of the lightly reinforced concrete walls(Lu, Henry, Gultom, & Ma, 2017), (Lu, Gultom, Ma, & Henry, 2018). Both walls were designed as 1.4 m long, 2.8 m high and 150 mm thick and represented a 40-50% scale version of multi-storey flexure-dominant RC wall. The limited ductile designed wall C1 with the distributed reinforcement satisfied with requirement of NZS 3010:2006-A2 (NZS 3101-A2, 2011) and the ductile designed wall M5 with additional reinforcement at the ends of walls satisfied the requirements in NZS 3010:2006-A3 (NZS 3101-A3, 2017)

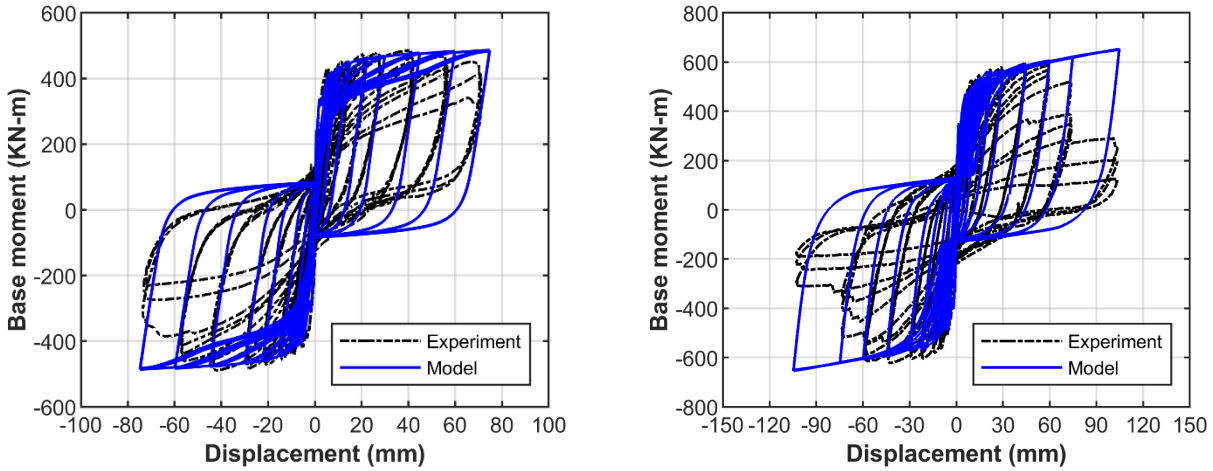

(a) Wall C1 **(b) Wall M5**

Figure 3: Comparison of the proposed model and experiment Wall C1 & M5

The objective of the numerical models was to validate the approach for capturing the global hysteresis behaviour for the lightly reinforced walls. The wall models consisted of four equal length DBE element up

the height of the wall. Although the walls were designed to be flexure controlled, previous research indicated that shear displacements can account for around 10% of the total lateral displacement (Dazio, Beyer, & Bachmann, 2009), (Lu, Gultom, Ma, & Henry, 2018). In order to describe the real response of the wall, the shear spring merged approach was applied into the model where the zero-length element was set at the ¼ and ¾ height of the wall. As shown by the comparison in Figure **3**, good agreement between the simulated and experimental results was observed. For both walls C1 and M5, strength degradation occurred due to buckling and subsequence fracture of the vertical reinforcement under the cyclic loading. Whereas the constitutive laws for the reinforcement model ignored the softening stage during buckling, thus leading to continuous strength increase. Despite this, the walls hysteresis response were still captured with sufficient accuracy by the numerical models.

3.3 Wall A10 (NZS 3101:2006-A2)

Wall A10 was part of the test program to investigate the seismic performance for more heavily reinforced concrete walls designed in accordance with NZS 3101:2006-A2 (Shegay, 2019). The test wall was 2.8 m long, 3.5 m high and 200 mm thick to represent the seismic behaviour of the lower two stories in an 8-storey archetypical office building located in Wellington.

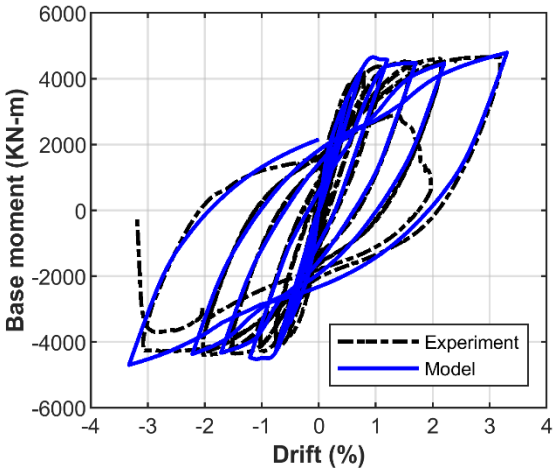

Figure 4: Comparison of the proposed model and the experiment Wall A10

The objective of the model was to validate the technique for capturing the global hysteresis behaviour of heavily reinforcement walls section that was commonly representative for the lower plastic hinge regions in tall buildings. In order to simplify the loading protocol for modelling, the entire 8-storey height wall was constructed in the model with the apportionment of inverted triangle lateral loading at each storey up the full wall height. The performance of the lower two stories was recorded corresponding with the test wall. Compared with the experimental data, the hysteresis behaviour calculated by the model showed good agreement, as shown in Figure 4. It was concluded that the proposed model technique was suitable to predict the response of walls with a range of reinforcement contents.

4 FUTURE WORK

Based on the calibrated models presented in the previous section, the fiber element with shear spring model formulation will be used to investigate the lateral load response of a 10-storey tall wall designed in accordance with ACI 318-19. The dimensions of the modelled wall were 3.5 m high for each storey, 35 m high for the entire wall, 4.6 m long and 210 mm thick, which was based on the web region from an existing 10-storey archetypical core wall model (Panagiotou & Restrepo, 2009). The wall designed with a specified concrete strength of 43 MPa and calculated tensile strength of 3.6 MPa. The properties of Grade 60

reinforcement were 480 MPa yield strength and 730 ultimate strength, as recommended by tall building design guidelines (Los Angeles Tall Buildings Structural Design Council, 2017). ACI 318-19 includes new minimum vertical reinforcement provisions that require additional vertical reinforcement extending from the critical section distance not less than the greater of l_w and $M_u/3V_u$, where l_w is the wall length and M_u/V_u is the shear span ratio. In order to investigate the terminating additional vertical reinforcement impact on flexural demand, the 10-storey rectangular wall designed with the minimum longitudinal reinforcement contents will be compared the response with the termination length of $M_u/4V_u$ (2 storeys), $M_u/3V_u$ (3 storeys), $M_u/2V_u$ (4 storeys) and full height (10 storeys).

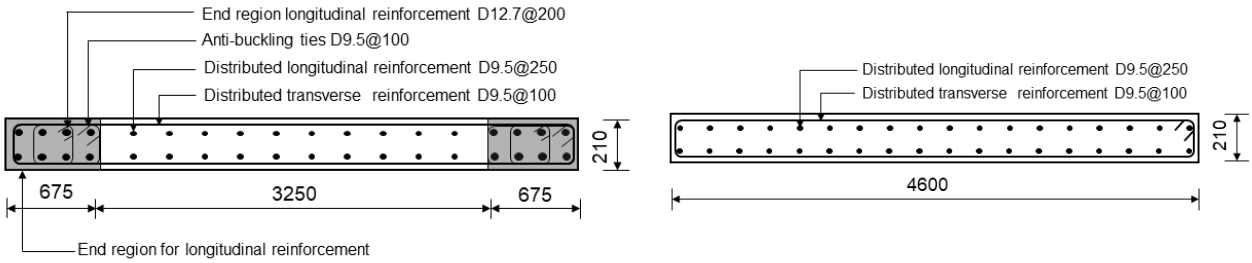

(a) Section details for bottom two storeys wall **(b) Section details for the upper storeys wall**

Figure 5: Section details of 10-storey wall

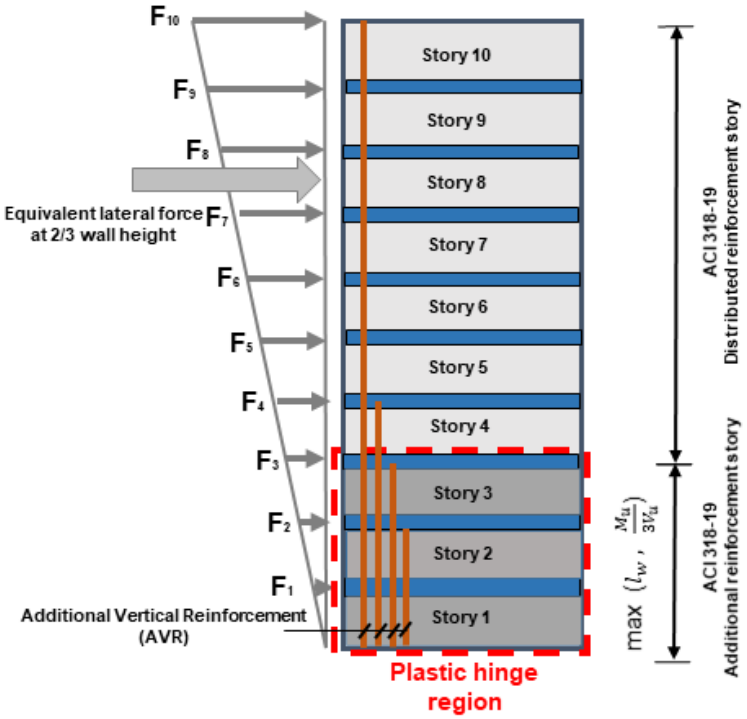

Figure 6: Loading protocol for a 10-storey wall designed by ACI 318-19

Ductile design with the additional vertical reinforcement was required in ACI 318-19 to ensure the well deformation capacity for the wall section within the plastic hinge region. The wall section beyond the base plastic hinge region was assumed to remain the elastic behaviour under the earthquake. Thus the distributed vertical reinforcement was required for the limited ductile design. For the wall section in the plastic hinge region, the minimum end zone longitudinal reinforcement ratio was required 0.68% ($\sqrt{f_c'}/2f_y$), leading to

two layers of 4 * D12.7 (#4) bars (diameter = 12.7 mm) placed at 200 mm within the end region with the reinforcement ratio of 0.71%, and the distributed minimum longitudinal reinforcement ratio was required 0.25% in the web region, resulting two layers of 12 * D9.5 (#3) bars (diameter = 9.5 mm) placed at 250 mm centres over the wall length with the reinforcement ratio of 0.25%, as shown in Figure 6a. For the wall section outside the plastic hinge region, the distributed minimum longitudinal reinforcement ratio was required 0.25% for the entire wall section, resulting two layers of 18 * D9.5 (#3) bars (diameter = 9.5 mm) placed at 250 mm centres over the wall length with the reinforcement ratio of 0.25%, as shown in Figure 6b. The transverse reinforcement and anti-buckling ties were designed to meet the construction requirement. The imposed axial load was assumed as 0.3% $f_c' A_g$ for each storey. The 10-storey wall be loaded with an inverted triangular lateral load pattern up the entire wall height, as shown in Figure 6.

5 SUMMARY

The current standards design walls with the ductile requirement at the plastic hinge storeys and no special ductile requirement at upper storeys. The efficient modelling method had been calibrated with the experimental tests with a range of vertical reinforcement contents. Modelling of a 10-storey wall designed in accordance with ACI 318-19 minimum reinforcement requirement is ongoing to investigate the impact of terminating additional longitudinal reinforcement on the lateral load response. According to the presented numerical analysis, the following preliminary conclusions can be drawn:

- For the walls designed with the minimum longitudinal reinforcement requirement, both ultimate strain and strain hardening slope regularisation of reinforcement properties are essential to capture the behaviour of lightly reinforced walls controlled by tension failure.
- The four equal-length DBE divisions with the shear springs can provide a relatively accurate estimation for the walls with a range of vertical reinforcement contents.

Future development of this research will include:

1. Extend the modelling to the non-rectangular wall section and analyse the core wall system performance.
2. Time history analysis for tall walls to investigate the reinforcement content impact on walls behaviour under the dynamic response.

ACKNOWLEDGEMENTS

The authors wish to acknowledge the Chinese Scholarship Council and the University of Auckland to provide financial support for this research program. In addition, the authors are grateful for the contribution from Dr Lu Yiqiu, Dr Alex Shegay and Dr Ash. Puranam for kindly sharing the experimental data.

REFERENCES

ACI Committee 318. 2014. *Building Code Requirements for Structural Concrete(ACI 318-14)* (Vol. 11).

Arabzadeh, H., & Galal, K. 2017. Seismic Collapse Risk Assessment and FRP Retrofitting of RC Coupled C-Shaped Core Walls Using the FEMA P695 Methodology. *Journal of Structural Engineering*, *143*(9),

ASCE 41-06. 2007. Seismic Rehabilitation of Existing Buildings. *American Society of Civil Engineers.*

Beyer, K. 2007. Seismic design of torsionally eccentric buildings with U-shaped RC Walls. *Rose School.*

Dazio, A., Beyer, K., & Bachmann, H. (2009). Quasi-static cyclic tests and plastic hinge analysis of RC structural walls. *Engineering Structures*, *31*(7), 1556–1571.

Encina, E., & Henry, R. 2015. Preliminary investigation of elongation in RC walls. *2015 NZSEE Conference*

fib Bulletin 65. 2012. *fib Model Code 2010 Volume 1. the International Federation for Structural Concrete (fib).*

Filippou, F. C., Popov, E. P., & Beryero, V. V. 1983. Effects of Bond Deterioration on Hysteretic Behavior of Reinforced Concrete Joints. *Earthquake Engineering Research Center, University of California, Berkeley*

J， Coleman;, & Spacone, E. 2001. Localization Issues in Force-Based Frame Elements. *Journal of Structural Engineering*, *127*(November), 1257–1265.

Los Angeles Tall Buildings Structural Design Council. 2017. *An Alternative Procedure for Seismic Analysis and Design of Tall Buildings Located in the Los Angeles Region*.

Lu, Y., Gultom, R. J., Ma, Q. Q., & Henry, R. S. 2018. Experimental validation of minimum vertical reinforcement requirements for ductile concrete Walls. *ACI Structural Journal, 115(4), 1115–1130.*

Lu, Y., Henry, R. S., Gultom, R., & Ma, Q. T. 2017. Cyclic Testing of Reinforced Concrete Walls with Distributed Minimum Vertical. *Journal of Structural Engineering*, *143*(5).

Marafi, N. A., Ahmed, K. A., Lehman, D. E., & Lowes, L. N. 2019. Variability in Seismic Collapse Probabilities of Solid- and Coupled-Wall Buildings. *Journal of Structural Engineering*, *145*(6),

NZS 3101-A2. 2011. NZS 3101-A2: Concrete structures standard. Wellington, New Zealand, Standards New Zealand.

NZS 3101-A3. 2017. NZS 3101-A3: Concrete structures standard. Wellington, New Zealand Standards New Zealand.

Orakcal, K., Massone, L. M., & Wallace, J. W. 2006. Analytical modeling of reinforced concrete walls for predicting flexural and coupled-shear-flexural responses. *Pacific Earthquake Engineering Research (PEER) Center*, (October), 228.

Panagiotou, M., & Restrepo, J. I. 2009. Dual-plastic hinge design concept for reducing higher-mode effects on high-rise cantilever wall buildings. *Earthquake Engineering and Structural Dynamics*, *38(12), 1359–1380.*

Priestley, M. J. N., Calvi, G. M., & Kowalsky.M.J 2007. Displacement-Based Seismic Design of Structures. *IUSS Press.*

Pugh, J. S. 2012. Numerical Simulation of Walls and Seismic Design Recommendations for Walled Buildings. *PhD Thesis, University of Washington*.

Puranam, A., & Pujol, S. 2017. Minimum Flexural Reinforcement in Reinforced Concrete Walls. *16th World Conference on Earthquake, 16WCEE 2017, 1–10.*

R.W.G.Blakeley, R.C.Cooney, & L.M.Negget. 1975. Seismic Shear Loading At Flexural Capacity in Cantilever Wall Structures. *Bulletin of the New Zealand National Society for Earthquake Engineering*, *8(December).*

Scott, M. H., & Fenves, G. L. 2006. Plastic Hinge Integration Methods for Force-Based Beam–Column Elements. *Journal of Structural Engineering*, *132(2), 244–252.*

Scott, M. H., & Ryan, K. L. 2013. Moment-rotation behavior of force-based plastic hinge elements. *Earthquake Spectra*.

Shegay, A. V. (2019). Seismic Performance of Reinforced Concrete Walls Designed For Ductility. *The University of Auckland.*

Spacone;, E., Filippou, F. C., & Taucer, F. F. 1996. Fibre Beam-Column Model for Non-Linear Analysis of R/C Frames: Part I. Formulation. *Earthquake Engineering & Structural Dynamics, 25(7), 711–725.*

Yang, Q. 2019. New Zealand Wall Design (NZWD) *https://github.com/qyan327/RC-wall-design*

Yassin Mohd, M. H. 1994. Nonlinear analysis of prestressed concrete structures under monotonic and cyclic loads. *University of California, Berkeley.*